

**Weak measurements and quantum weak values for NOON states**L. Rosales-Zárate,<sup>1,2</sup> B. Opanchuk,<sup>2</sup> and M. D. Reid<sup>2</sup><sup>1</sup>*Centro de Investigaciones en Óptica A.C., León, Guanajuato 37150, Mexico*<sup>2</sup>*Centre for Quantum and Optical Science, Swinburne University of Technology, Melbourne 3122, Australia*

(Received 18 November 2017; published 26 March 2018)

Quantum weak values arise when the mean outcome of a weak measurement made on certain preselected and postselected quantum systems goes beyond the eigenvalue range for a quantum observable. Here, we propose how to determine quantum weak values for superpositions of states with a macroscopically or mesoscopically distinct mode number, that might be realized as two-mode Bose-Einstein condensate or photonic NOON states. Specifically, we give a model for a weak measurement of the Schwinger spin of a two-mode NOON state, for arbitrary  $N$ . The weak measurement arises from a nondestructive measurement of the two-mode occupation number difference, which for atomic NOON states might be realized via phase contrast imaging and the ac Stark effect using an optical meter prepared in a coherent state. The meter-system coupling results in an entangled cat-state. By subsequently evolving the system under the action of a nonlinear Josephson Hamiltonian, we show how postselection leads to quantum weak values, for arbitrary  $N$ . Since the weak measurement can be shown to be minimally invasive, the weak values provide a useful strategy for a Leggett-Garg test of  $N$ -scopic realism.

DOI: [10.1103/PhysRevA.97.032123](https://doi.org/10.1103/PhysRevA.97.032123)**I. INTRODUCTION**

It would seem impossible that the outcome of a measurement of a quantum observable could yield an average that is outside the eigenvalue range associated with the observable spectra. Yet such a paradoxical situation was predicted by Aharonov, Albert, and Vaidman in their paper entitled “How the result of a measurement of a component of the spin of a spin 1/2 particle can turn out to be 100” [1]. The situation arises for the outcomes of so-called *weak measurements* [1–15]. Weak measurements are measurements that couple weakly to the quantum system being measured, so as to give a minimal disturbance to that system. In their paper, Aharonov, Albert, and Vaidman explained how one can perform a weak measurement of the spin  $\sigma_z$  of a spin-1/2 particle and obtain a result where the average ( $\langle\sigma_z\rangle$ ) exceeds 100.

The paradoxical measurement outcomes that lead to the strange predictions are called quantum *weak values* [1–15]. Weak values arise as the outcomes of weak measurements on systems prepared by preselection and postselection. The weak values are created by the phenomenon of quantum interference and have been used to interpret quantum mechanics in scenarios where quantum interference leads to counterintuitive predictions [3,11,12,16]. The weak measurements and weak values also have practical applications, for precision measurements and in providing a means to monitor a quantum system with a demonstrably minimal disturbance to that system [3]. For this reason, weak measurements have been used to test Leggett and Garg’s form of macrorealism and microrealism in experiments that show violation of Leggett-Garg inequalities [3,7–15].

The topic of weak values has attracted much interest. The experimental prediction of Aharonov, Albert, and Vaidman has been realized at the level of a spin-1/2 system by Pryde *et al.*, who demonstrated weak values for a photonic qubit [4]. Their weak measurement scheme involved a single photon interacting with the photonic qubit in a process that created an

entangled state. The experiment detected weak values outside the eigenvalue range for the spin  $\sigma_z$  defined by the polarization of the photon.

Goggin *et al.* applied the weak measurement of Pryde *et al.* in an experiment that demonstrated failure of the Leggett-Garg premises for the microscopic photonic system [9]. The Leggett-Garg premises are: first, that the system must be, prior to any measurement, in one spin state or the other (“up” or “down”); and, second, that a measurement can in principle be performed on the system to determine which spin state the system is in, without interfering with the subsequent two-state spin dynamics [17]. The measurement perceived by Leggett and Garg is called the noninvasive measurement. The connection between quantum weak values and the violation of Leggett-Garg inequalities was formalized by Ruskov *et al.*, Jordan *et al.*, and Williams and Jordan, who showed that if a weak measurement is used as the noninvasive measurement, then the violation of the inequalities is associated with the appearance of weak values [7,8].

While there has been much progress and insight gained into quantum mechanics using weak values, to date this has not been fully extended to mesoscopic or macroscopic systems [18,19]. Weak measurements have been used to probe quantum states and to demonstrate violation of Leggett-Garg inequalities in superconducting circuits [10,14]. Williams and Jordan proposed the implementation of a weak measurement with quantum weak values for solid-state qubits, that could be generalized to macroscopic superconducting systems based on the assumption of a macroscopic qubit [8]. This was followed by an experimental observation of weak values for a superconducting circuit [6]. However, to our knowledge, there has been no experimental report of quantum weak values for superposition states involving even moderate numbers of photons or atoms. The potential for weak values in mesoscopic atomic systems was illustrated by Huang and Agarwal [20], who studied the quantum interference arising from two close-lying atomic co-

herent states, and showed how the phase shift due to the quantum interference can be amplified using weak measurements.

In this paper, we consider a quantum weak-value gedanken experiment that applies to NOON states, given as [21,22]

$$|\text{NOON}\rangle = d_N |N\rangle_a |0\rangle_b + d_0 |0\rangle_a |N\rangle_b. \quad (1)$$

Here  $|N\rangle_a$  and  $|N\rangle_b$  are number states for two atomic or photonic modes (that we denote by  $a$  and  $b$ ) and  $d_0$  and  $d_N$  are probability amplitudes. We give a model for a quantum measurement of the two-level spin of the two-mode quantum system, the two-level spin being defined as  $\hat{S}_z/N$  where  $\hat{S}_z$  is the two-mode Schwinger operator for the occupation number difference between the two modes. The interaction due to the measurement couples a meter system to the quantum system, with a coupling strength  $\gamma$ , creating an entanglement between the meter and quantum system [23,24]. For a Bose-Einstein condensate (BEC), this can be realized as a nondestructive phase contrast imaging measurement based on the ac Stark effect [24]. In the limit of large  $\gamma$ , a final homodyne detection would collapse the quantum system into a state of definite spin, thus completing the von Neumann measurement process. For weak coupling  $\gamma$ , this collapse does not take place and the system is minimally disturbed by the measurement. For all  $\gamma$ , however, the average spin  $\langle \hat{S}_z \rangle$  can be correctly evaluated.

Similar to Ref. [8], we demonstrate weak values by considering a unitary evolution from a time  $t_2$  to a time  $t_3$  that rotates the probability amplitudes associated with the NOON state, while retaining the two-state nature of the system. The weak values are obtained by postselecting the result for the measurement at time  $t_2$ , given a result at time  $t_3$ . We show that the two-state NOON unitary evolution can be realized to an excellent approximation by the Hamiltonian used to model two trapped Bose-Einstein condensates with a Josephson coupling, in certain parameter regimes that include nonlinear effects [25–32]. In fact, by solving the two-mode nonlinear Josephson Hamiltonian, we find that weak values are predicted over a range of parameter values, including where the system is not the ideal NOON state at time  $t_3$ , but rather a superposition of two mesoscopically distinguishable states with a range of outcomes for  $\hat{S}_z$ . This suggests an experimental realization to be feasible.

The proposed weak measurement opens a way to test mesoscopic realism using weak values and NOON states. This is because a measurement can be constructed for the system at a time  $t_2$  that can be justified as noninvasive for the test of the Leggett-Garg inequality. We give details of how one can experimentally demonstrate the noninvasiveness of the weak measurement, and give predictions for such an experiment, confirming the connection between the observation of weak values and the violation of the Leggett-Garg inequalities for a macroscopic superposition. A preliminary description of this proposal for a Leggett-Garg test of macrorealism and/or mesorealism has been presented in Ref. [33].

The paper is organized as follows. In Secs. II and III we give details of the model for the weak measurement of the spin  $\hat{S}_z/N$ . In Sec. IV we show how the weak values emerge for the postselected spin at time  $t_2$ . The Leggett-Garg test of mesorealism and the Josephson Hamiltonian is explained in Sec. V. In Sec. VI, we give predictions for weak values and violation of Leggett-Garg inequalities using the Josephson model in the nonideal case.

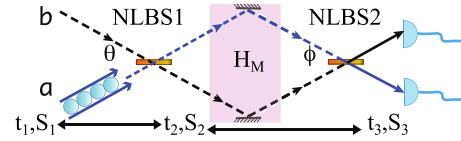


FIG. 1. Schematic of an experiment to detect weak values for NOON states: A system is prepared in a NOON state at the time  $t_2$ . Here, the preparation involves  $N$  bosons in a mode  $a$  incident on a nonlinear medium at time  $t_1$  as described in Secs. IV and V. A second mode  $b$  is initially in a vacuum state. The nonlinear interaction is modelled by the Hamiltonian  $H_I$  given by Eq. (35). This interaction is symbolized by the nonlinear beam splitter NLBS1, where  $\theta$  denotes the time of interaction  $t_2 - t_1$  in scaled units (see main text). The spin  $S_i$  is defined to be  $+1$  or  $-1$  according to the sign of the mode number difference at time  $t_i$ . Once the NOON state is prepared by the first nonlinear beam splitter, a weak measurement  $M$  of the spin  $S_2$  takes place at time  $t_2$ , as depicted by the purple shading. The measurement interaction is described by the Hamiltonian  $H_M$  given by Eq. (3). After the measurement, the system evolves under the action of  $H_I$  for a time denoted  $\phi$  (in scaled units), as symbolized by the second nonlinear beam splitter NLBS2. Assuming a near-instantaneous measurement  $M$ , the time  $\phi$  is  $t_3 - t_2$  in scaled units. After the second interaction, a strong measurement of  $S_3$  takes place at time  $t_3$ . Weak values are observed when the value  $\langle S_2 \rangle_{S_3=1}$  of the spin  $S_2$  conditional on the result  $S_3 = 1$  exceeds the eigenvalue bounds given by  $|\langle S_2 \rangle| \leq 1$ .

## II. A NONDESTRUCTIVE MEASUREMENT OF SPIN

We consider a two-mode bosonic system. The boson creation and destruction operators for the modes are  $\hat{a}^\dagger, \hat{a}$  and  $\hat{b}^\dagger, \hat{b}$  respectively and we will denote the modes by the symbols  $a$  and  $b$ . The operators  $\hat{J}_z = (\hat{a}^\dagger \hat{a} - \hat{b}^\dagger \hat{b})/2$ ,  $\hat{J}_x = (\hat{a}^\dagger \hat{b} + \hat{b}^\dagger \hat{a})/2$ ,  $\hat{J}_y = (\hat{a}^\dagger \hat{b} - \hat{b}^\dagger \hat{a})/2i$ ,  $\hat{N} = \hat{a}^\dagger \hat{a} + \hat{b}^\dagger \hat{b}$  are the Schwinger spin operators (we take  $\hbar = 1$ ). For convenience, we introduce the population (number) difference operator  $\hat{S}_z = 2\hat{J}_z$ . Thus,

$$\hat{S}_z = \hat{a}^\dagger \hat{a} - \hat{b}^\dagger \hat{b} = \hat{n}_a - \hat{n}_b, \quad (2)$$

where  $\hat{n}_a = \hat{a}^\dagger \hat{a}$  and  $\hat{n}_b = \hat{b}^\dagger \hat{b}$ . The objective is to give a (noninvasive) measurement of the spin  $\hat{J}_z$  (or  $\hat{S}_z$ ) of the two-mode system. The two-mode system could be a Bose-Einstein condensate (BEC) in a double-well potential [25–29,32], a two-component BEC where each component is associated with a distinct atomic level and a distinct mode [31], or a two-mode photonic state [21]. In the weak-value gedanken experiment that we discuss in Sec. III, a weak measurement is to be performed at a time  $t_2$  (Fig. 1).

We consider the nondestructive measurement  $M$  of  $\hat{J}_z = \hat{S}_z/2$ , described by the measurement Hamiltonian [23,24]

$$H_M = \hbar G \hat{S}_z \hat{n}_c / 2. \quad (3)$$

The measurement is performed by coupling the two-mode system to an optical field. The field is modelled as a single mode with boson operator  $\hat{c}$  and number operator  $\hat{n}_c = \hat{c}^\dagger \hat{c}$ . The optical “meter” field is prepared in a coherent state  $|\gamma\rangle$  and coupled to the two-mode system for a time  $\tau$ . The measurement interaction is modelled by the Hamiltonian  $H_M$  where  $G$  is the coupling constant.

In this paper, we consider systems that are eigenstates of the total number  $\hat{N} = \hat{a}^\dagger \hat{a} + \hat{b}^\dagger \hat{b}$ . We denote the total number of bosons (atoms or photons) as  $N$ . Assuming a pure state,

the general form of the two-mode state immediately prior to measurement is

$$|\psi\rangle_{\text{in}} = \sum_{m=0}^N d_m |m\rangle_a |N-m\rangle_b, \quad (4)$$

where  $d_m$  are probability amplitudes. As a first step, we consider how to measure  $\langle \hat{S}_z \rangle$  of this state. The output *after* the measurement is given by

$$\begin{aligned} |\psi\rangle_{\text{out}} &= e^{-iH_M\tau/\hbar} \sum_m d_m |m\rangle_a |N-m\rangle_b |\gamma\rangle_c \\ &= \sum_{m=0}^N d_m |m\rangle_a |N-m\rangle_b |\gamma e^{iG\tau(N-2m)}\rangle_c. \end{aligned} \quad (5)$$

The output state after a measurement interaction time  $\tau = \pi/2NG + 2\pi K$  where  $K$  is a nonnegative integer is therefore

$$|\psi\rangle_{\text{out}} = \sum_{m=0}^N d_m |m\rangle_a |N-m\rangle_b |\gamma e^{i\pi(N-2m)/2N}\rangle_c. \quad (6)$$

Homodyne detection on the optical system enables measurement of the meter quadrature phase amplitude  $\hat{p} = (\hat{c} - \hat{c}^\dagger)/i$ . For  $\gamma$  large, the different values of  $\hat{S}_z$  are measurable by outcomes for  $\hat{p}$  and the two-mode system after the homodyne measurement collapses to a state of definite  $\hat{S}_z$ . This is the limit of a strong, projective measurement. More generally, for all values of  $\gamma$ , it can be shown based on the work by Ilo-Okeke and Byrnes [24] that

$$\langle \hat{S}_z \rangle = -\frac{1}{2\gamma} \langle \hat{p} \rangle. \quad (7)$$

The average of  $\hat{p}$  gives the value for the average of the Schwinger spin  $\hat{S}_z$  of the incident two-mode state. This relation is true for all values of  $\gamma$  including the limit where  $\gamma \rightarrow 0$ , called the weak measurement limit. A detailed analysis of the measurement model as applied to a BEC system is given in Ref. [24].

### III. A WEAK MEASUREMENT ON NOON STATES

Our interest in this paper is where the incident state (4) before the measurement  $M$  is a macroscopic or mesoscopic superposition state. Specifically, we consider the case where the two-mode system (4) is the ideal NOON state given by

$$|\psi\rangle_{\text{in}} = d_0 |0\rangle_a |N\rangle_b + d_N |N\rangle_a |0\rangle_b. \quad (8)$$

In this case, the outcome of the measurement  $\hat{S}_z$  is either  $N$  or  $-N$ . For later convenience, we suppose the measurement is made on the system at the time  $t_2$ , so that the state  $|\psi\rangle_{\text{in}}$  before the measurement is created at time  $t_2$  (Fig. 1). We define  $S_2$  to be the outcome of the normalized measurement  $\hat{S}$  defined as  $\hat{S} = \hat{S}_z/N$  at this time  $t_2$ . More generally, we define the measurement of  $\hat{S}$  at time  $t_i$  to be  $\hat{S}_i$  and the corresponding outcome to be  $S_i$ .

Where the input state (4) prior to the measurement  $M$  is the NOON state (8), the final state (6) after the measurement  $M$  can be written

$$|\psi\rangle = d_0 |0\rangle_a |N\rangle_b |i\gamma\rangle_c + d_N |N\rangle_a |0\rangle_b |i\gamma\rangle_c. \quad (9)$$

This state describes an entanglement of the two-mode quantum system with the meter field. The two outputs (the two-mode state and the meter field) are next spatially separated, and a measurement is then made of the quadrature  $\hat{p} = \frac{1}{i}(\hat{c} - \hat{c}^\dagger)$  of the meter field. For  $\gamma$  large, the two different values  $\pm N$  for  $\hat{S}_z$  (and hence of  $S_2$ ) are measurable by the different sign of the outcomes for  $\hat{p}$ . The two-mode system after the homodyne measurement collapses to a state of definite  $\hat{S}_z$ , either the eigenstate  $|N\rangle_a |0\rangle_b$  with eigenvalue  $N$  or the eigenstate  $|0\rangle_a |N\rangle_b$  with eigenvalue  $-N$ .

A measurement of the meter quadrature  $\hat{p}$  thus yields a measurement of the spin  $S_2$ . We can evaluate  $\langle \hat{p} \rangle$  directly from (9) to give the relationship

$$\begin{aligned} \langle \hat{p} \rangle &= 2\gamma(|d_0|^2 - |d_N|^2) \\ &= -2\gamma \langle S_2 \rangle. \end{aligned} \quad (10)$$

Details are given in the Appendixes. Here we have used  $\langle S_2 \rangle = |d_N|^2 - |d_0|^2$ , which is the expectation value of  $S_2$  for the initial two-mode state (8). We see that  $\langle S_2 \rangle = -\frac{1}{2\gamma} \langle \hat{p} \rangle$  consistent with the general result (7) given in Ref. [24]. The average of  $\hat{p}$  will give the value for the average of the Schwinger spin of the incident two-mode state.

We suppose as in Fig. 1 that the measurement  $M$  takes place at a time  $t_2$ . The time  $t_1$  is reserved for earlier events that lead to the preparation of the NOON state at time  $t_2$ . We next consider that the two-mode state evolves for a time  $t$  under an interaction Hamiltonian  $H_I$ , and that a projective measurement is made at the later time  $t_3$ . The Hamiltonian is unspecified at this stage, except that it conserves the total particle number  $N$ . We will consider that the measurement time  $\tau$  is small compared to the later evolution time  $t$ , so that we take  $t = t_3 - t_2$ . Under the evolution due to  $H_I$ , the output state (6) [or (9)] produced immediately *after* the measurement at time  $t_2$  evolves to a new state at the time  $t_3$ . The Hamiltonian  $H_I$  is such that the two-mode state  $|m\rangle_a |N-m\rangle_b$  evolves to the state given by

$$\sum_n c_n^{(m)} |n\rangle_a |N-n\rangle_b, \quad (11)$$

where  $c_n^{(m)}$  are probability amplitude constants. The final output state including the meter field is

$$|\psi(t_3)\rangle = \sum_m d_m |\gamma e^{i\pi(N-2m)/2N}\rangle_c \sum_n c_n^{(m)} |n\rangle_a |N-n\rangle_b. \quad (12)$$

An experimentalist can measure  $S_3$  at the final time  $t_3$ . The experimentalist can also measure the outcome  $p$  of the measurement  $\hat{p}$  of the meter field, and obtain the correlation  $\langle p S_3 \rangle$ . We next evaluate  $\langle p S_3 \rangle$  and compare with  $\langle S_2 S_3 \rangle$ .

In this section, we take the case where just prior to the measurement at time  $t_2$  the two-mode system is in the NOON state (8). At time  $t_3$ , after measurement and after the subsequent evolution, the overall state is given by Eq. (12) which we simplify as

$$\begin{aligned} |\psi(t_3)\rangle &= d_0 |\gamma e^{+i\pi/2}\rangle_c \sum_n c_n^{(0)} |n\rangle_a |N-n\rangle_b \\ &\quad + d_N |\gamma e^{-i\pi/2}\rangle_c \sum_n c_n^{(N)} |n\rangle_a |N-n\rangle_b. \end{aligned} \quad (13)$$

We evaluate  $\langle pS_3 \rangle = \langle \psi(t_3) | pS_3 | \psi(t_3) \rangle$ . Using that

$$\langle S_2 S_3 \rangle = |d_N|^2 \left( - \sum_{n < N/2} |c_n^{(N)}|^2 + \sum_{n > N/2} |c_n^{(N)}|^2 \right) - |d_0|^2 \left( - \sum_{n < N/2} |c_n^{(0)}|^2 + \sum_{n > N/2} |c_n^{(0)}|^2 \right) \quad (14)$$

we find

$$\langle S_2 S_3 \rangle = - \frac{1}{2\gamma} \langle pS_3 \rangle. \quad (15)$$

Details of the calculation are given in the Appendixes. In summary, if immediately prior to measurement at time  $t_2$  the two-mode system is in the generalized NOON state (8), then we have confirmed the relation (15). This relation is true for all values of the measurement coupling strength  $\gamma$ . The weak measurement result where  $\gamma \rightarrow 0$  gives the same average as the strong (projective) measurement result (large  $\gamma$ ).

The expression (15) enables a weak measurement strategy to be employed for a Leggett-Garg test of macroscopic or mesoscopic realism. The measurement  $M$  at time  $t_2$  is made with a very small  $\gamma$ . The measurement can then be demonstrated to be noninvasive in the limit of  $\gamma \rightarrow 0$ . The average  $\langle pS_3 \rangle$  can be determined accurately by measuring over many trials, to give an accurate value for  $\langle S_2 S_3 \rangle$  that can be used to test the LG inequality. This approach was used in the experiment of Goggin *et al.*, for  $N = 1$  [9].

#### IV. WEAK VALUES

Continuing with the case where we make a weak measurement at time  $t_2$  on a NOON state (8), we now show how weak values emerge from the weak measurement (Fig. 1). In the case where the system is in a NOON state, the possible values of  $S_i$  at time  $t_i$  are  $+1$  and  $-1$ . Where the values of  $\hat{S}_z$  may be different to  $\pm N$  at time  $t_3$ , as is the case for nonideal states examined in Sec. VI, we define the binned measurement  $\tilde{S}_3$  made at time  $t_3$  to be  $+1$  if the outcome  $S_z$  of  $\hat{S}_z$  satisfies  $S_z \geq 0$ , and  $-1$  if  $S_z < 0$ . To realize quantum weak values, we will evaluate the mean value for  $S_2$ , given that the result  $+1$  is detected for the *postselected* measurement of  $\tilde{S}_3$ . Weak values are observed when the value  $\langle S_2 \rangle_{\tilde{S}_3=1}$  of the spin  $S_2$  conditional on the postselected result  $\tilde{S}_3 = 1$  exceeds the eigenvalue bounds given by  $|\langle S_2 \rangle| \leq 1$ . Although we do not adopt the convention here, to emphasize that the weak value is obtained by conditioning on the postselected result, we point out that the notation  ${}_1 \langle S_2 \rangle$  is often used.

At time  $t_3$ , after the weak measurement and after the subsequent evolution, the state is given by Eq. (12). We expand into a superposition of states giving a positive value of  $\tilde{S}_3$  and states giving a negative value of  $\tilde{S}_3$ :

$$\begin{aligned} |\psi(t_3)\rangle &= d_0 |\gamma e^{+i\pi/2}\rangle_c \sum_{n \geq N/2} c_n^{(0)} |n\rangle_a |N-n\rangle_b \\ &+ d_N |\gamma e^{-i\pi/2}\rangle_c \sum_{n \geq N/2} c_n^{(N)} |n\rangle_a |N-n\rangle_b \\ &+ d_0 |\gamma e^{+i\pi/2}\rangle_c \sum_{n < N/2} c_n^{(0)} |n\rangle_a |N-n\rangle_b \\ &+ d_N |\gamma e^{-i\pi/2}\rangle_c \sum_{n < N/2} c_n^{(N)} |n\rangle_a |N-n\rangle_b. \quad (16) \end{aligned}$$

Here we have allowed that a state more general than a NOON state may be generated at time  $t_3$ . An experimentalist can measure  $S_3$  at the final time  $t_3$  and postselect for the outcome  $\tilde{S}_3 = 1$ . Where the system at time  $t_3$  is in a NOON state, the postselection is conditional on  $S_3 = 1$ . The experimentalist can also measure  $\hat{p}$  of the meter field, and obtain the mean value for the outcomes  $p$  (and hence the inferred  $S_2$ ) conditional on the result  $\tilde{S}_3 = 1$ . We denote these conditional moments as  $\langle p \rangle_{\tilde{S}_3=1}$ , or  $\langle S_2 \rangle_{S_3=1}$ . We see that

$$\langle p \rangle_{\tilde{S}_3=1} = \frac{\int p P(p, S_3 \geq 0) dp}{P(S_3 \geq 0)}, \quad (17)$$

where

$$P(S_3 \geq 0) = \int P(p, S_3 \geq 0) dp. \quad (18)$$

Using the general state given in Eq. (16) we obtain

$$\begin{aligned} P(p, S_3 \geq 0) &= |d_0|^2 |\langle p | \gamma e^{+i\pi/2} \rangle|^2 \sum_{n \geq N/2} |c_n^{(0)}|^2 \\ &+ |d_N|^2 |\langle p | \gamma e^{-i\pi/2} \rangle|^2 \sum_{n \geq N/2} |c_n^{(N)}|^2 + \text{Int}, \quad (19) \end{aligned}$$

where

$$\begin{aligned} \text{Int} &= d_0^* d_N \langle \gamma e^{+i\pi/2} | p \rangle_c \langle p | \gamma e^{-i\pi/2} \rangle_c \sum_{n \geq N/2} c_n^{(0)*} c_n^{(N)} \\ &\times d_N^* d_0 \langle \gamma e^{-i\pi/2} | p \rangle_c \langle p | \gamma e^{+i\pi/2} \rangle_c \sum_{n \geq N/2} c_n^{(N)*} c_n^{(0)} \quad (20) \end{aligned}$$

is a quantum interference term. In fact

$$\langle p | \gamma e^{\pm i(\pi/2)} \rangle = \frac{\exp(-\frac{p^2}{4} + \frac{\gamma^2 e^{\pm i\pi}}{2} - \frac{\gamma^2}{2} - i p \gamma e^{\pm i(\pi/2)})}{(2\pi)^{1/4}} \quad (21)$$

and  $|\langle p | \gamma e^{\pm i(\pi/2)} \rangle|^2 = \frac{e^{-(p/\sqrt{2} - \sqrt{2}\gamma)^2}}{\sqrt{2\pi}}$ . Hence we can evaluate the conditional moments once we specify the evolution during the time from  $t_2$  to  $t_3$ .

In the next section, we consider an evolution  $H_I$  that gives rise to a violation of a Leggett-Garg inequality. We will restrict to this case. We thus consider the interaction Hamiltonian  $H_I$  defined in Sec. V that evolves an initial state  $|0\rangle_a |N\rangle_b$  at time  $t_2$  into the state

$$\cos(t_3 - t_2) |0\rangle_a |N\rangle_b + i \sin(t_3 - t_2) |N\rangle_a |0\rangle_b \quad (22)$$

at the later time  $t_3$ . Here time  $t_i$  is expressed in suitably scaled units, which will be defined in the next section. The interaction also evolves the state  $|N\rangle_a |0\rangle_b$  at time  $t_2$  into the state

$$i \sin(t_3 - t_2) |0\rangle_a |N\rangle_b + \cos(t_3 - t_2) |N\rangle_a |0\rangle_b \quad (23)$$

defined at time  $t_3$ . Hence we substitute in the expression (16)

$$\begin{aligned} c_0^{(0)} &= \cos(t_3 - t_2), \\ c_N^{(0)} &= i \sin(t_3 - t_2), \\ c_0^{(N)} &= i \sin(t_3 - t_2), \\ c_N^{(N)} &= \cos(t_3 - t_2). \quad (24) \end{aligned}$$

All other coefficients are zero. In this case,  $\tilde{S}_3 = S_3$  since an ideal NOON state is created at time  $t_3$ . Using Eq. (17), we find

$$P(p, S_3 \geq 0) = \frac{|d_0|^2 |c_N^{(0)}|^2}{\sqrt{2\pi}} e^{-(p/\sqrt{2}-\sqrt{2}\gamma)^2} + \frac{|d_N|^2 |c_N^{(N)}|^2}{\sqrt{2\pi}} e^{-(p/\sqrt{2}+\sqrt{2}\gamma)^2} + \text{Int.} \quad (25)$$

Hence

$$\int p P(p, S_3 \geq 0) dp = 2\gamma (|d_0|^2 |c_N^{(0)}|^2 - |d_N|^2 |c_N^{(N)}|^2) = -\gamma \cos^2 \theta, \quad (26)$$

where we note the interference terms do not contribute to this term, since  $\int_{-\infty}^{\infty} \exp(-\frac{p^2}{2} - 2\gamma^2) p dp = 0$ . Also,

$$P(S_3 \geq 0) = |d_0|^2 |c_N^{(0)}|^2 + d_0^* d_N c_N^{(0)*} c_N^{(N)} e^{-2\gamma^2} + d_N^* d_0 c_N^{(N)*} c_N^{(0)} e^{-2\gamma^2} + |d_N|^2 |c_N^{(N)}|^2 \quad (27)$$

which simplifies to

$$P(S_3 \geq 0) = \frac{1}{2} (1 - \sin \theta e^{-2\gamma^2}). \quad (28)$$

We find

$$\langle S_2 \rangle_{S_3=1} = -\frac{1}{2\gamma} \langle p \rangle_{S_3=1} = \frac{\cos \theta}{1 - \sin \theta e^{-2\gamma^2}}. \quad (29)$$

The form of this result agrees with that derived by Williams and Jordan, based on a similar two-state evolution and assuming a stroboscopic “kicked” weak quantum nondemolition (QND) measurement [8,34].

As one example that is relevant to tests of Leggett-Garg inequalities, we consider where the initial state prepared at time  $t_2$  is a generalized NOON state with amplitudes  $d_N = \cos(\theta/2)$  and  $d_0 = i \sin(\theta/2)$ . We select  $\theta = \pi/3$  and  $t_3 - t_2 = \pi/4$ . The limits of  $\langle S_2 \rangle_{S_3=1}$  for  $\gamma \rightarrow 0$  and  $\gamma \rightarrow \infty$  are then 3.73 and 0.5 respectively. The threshold for the weak value where  $\langle S_2 \rangle_{S_3=1} > 1$  is  $\gamma < \gamma_0$  given by  $\gamma_0 = 0.5241$ . In Fig. 2 we plot the value  $\langle S_2 \rangle_{S_3=1}$  versus  $\gamma$ . Weak values that are outside the eigenvalue range of  $|\langle S_2 \rangle_{S_3=-1}| \leq 1$  are evident for where  $\gamma < \gamma_0$ .

In a similar fashion, we calculate the prediction for  $\langle S_2 \rangle_{S_3=-1}$ . Calculation gives

$$\int p P(p, S_3 < 0) dp = 2\gamma (|d_0|^2 |c_0^{(0)}|^2 - |d_N|^2 |c_0^{(N)}|^2) \quad (30)$$

and

$$P(S_3 < 0) = |d_0|^2 |c_0^{(0)}|^2 + |d_N|^2 |c_0^{(N)}|^2 + d_0^* d_N c_0^{(0)*} c_0^{(N)} e^{-2\gamma^2} + d_N^* d_0 c_0^{(N)*} c_0^{(0)} e^{-2\gamma^2} \quad (31)$$

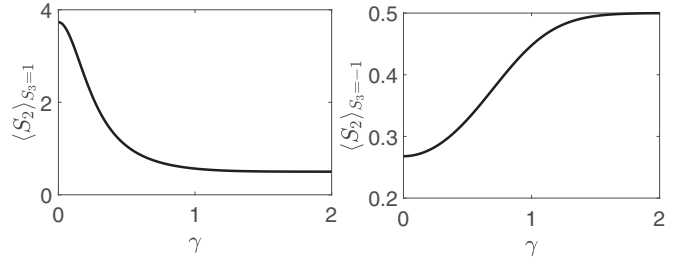


FIG. 2. Weak values for NOON states: The measured value of  $\langle S_2 \rangle_{S_3=1}$  and  $\langle S_2 \rangle_{S_3=-1}$  versus the measurement strength  $\gamma$  for  $\theta = t_2 - t_1 = \pi/3$  and  $\phi = t_3 - t_2 = \pi/4$ . The predictions for  $\langle S_2 \rangle_{S_3=1}$  show values outside the eigenvalue range bounded by  $\pm 1$ , for all  $\gamma < 0.5241$ .

leading to

$$\langle S_2 \rangle_{S_3=-1} = -\frac{1}{2\gamma} \langle p \rangle_{S_3=-1} = \frac{\cos \theta}{1 + \sin \theta e^{-2\gamma^2}}. \quad (32)$$

For the choice  $\theta = \pi/3$ , we find  $\langle S_2 \rangle_{S_3=-1} < 0.5$  for all  $\gamma$ , implying no weak value prediction for these parameters.

## V. LEGGETT-GARG TEST USING WEAK MEASUREMENTS

One may consider a Leggett-Garg test of macroscopic realism using NOON states and the weak measurements proposed in this paper. Leggett and Garg proposed to test macroscopic realism, by considering a two-state system where the two states are in some sense “macroscopically distinct,” e.g., a cat that is dead or alive [17]. Leggett and Garg defined two premises that embody the meaning of macroscopic realism. The two premises are summarized in the Introduction.

Leggett and Garg (LG) showed how the two premises [referred to as macrorealism (MR)] constrain the dynamics of a two-state system. Considering three successive times  $t_3 > t_2 > t_1$ , the variable  $S_i$  denotes which of the two states the system is in at time  $t_i$ , the respective two states being denoted by  $S_i = +1$  or  $-1$ . The Leggett-Garg premises imply the Leggett-Garg inequality [8,17]

$$\langle S_1 S_2 \rangle + \langle S_2 S_3 \rangle - \langle S_1 S_3 \rangle \leq 1. \quad (33)$$

Defining the parameter  $LG \equiv \langle S_1 S_2 \rangle + \langle S_2 S_3 \rangle - \langle S_1 S_3 \rangle$ , the Leggett-Garg inequality is also expressible as  $-3 \leq LG \leq 1$ . It is also possible to define the “no disturbance” or “no signaling in time” condition given by the equality

$$d_\sigma = \langle S_3 | \sigma \rangle_M - \langle S_3 | \sigma \rangle = 0. \quad (34)$$

Recent work shows that this condition is also implied by the Leggett-Garg macrorealism premises, where  $M$  represents the noninvasive measurement [35,36]. Here  $\langle S_3 | \sigma \rangle_M$  (and  $\langle S_3 | \sigma \rangle$ ) is the expectation value of  $S_3$  given that the measurement  $M$  is performed (or not performed) at time  $t_2$ , conditional on the system being prepared in a state denoted by  $\sigma$  at time  $t_1$ . The Leggett-Garg inequalities are predicted to be violated for quantum systems [10,17].

Figure 1 illustrates the proposed Leggett-Garg experiment based on the NOON states and weak measurement. The

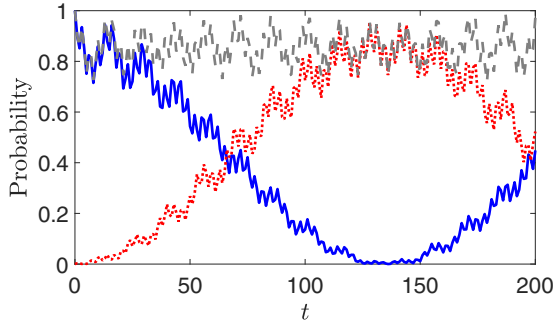


FIG. 3. Near-ideal two-state dynamics: We show the mesoscopic two-state oscillation predicted for the Hamiltonian  $H_I$  with  $N = 5$  and  $g/\kappa = 2$  and time  $t$  is in units of  $\kappa^{-1}$ . The blue solid (red dotted) line is the probability that 5 (0) bosons are found in the mode  $a$ , upon measurement of the number  $\hat{n}_a$  at time  $t$ . The black dashed line gives the sum of the two probabilities.

system at time  $t_1$  is prepared in a state with definite spin  $S_1 = 1$ . The system we consider evolves at time  $t_2$  to a NOON state (8). The measurement  $M$  given by (3) is made on this state at time  $t_2$ . The measurement  $M$  can be made as a weak measurement, or as a strong projective measurement, depending on the value of  $\gamma$ . In fact because the state at time  $t_1$  is deterministically prepared in the state with positive spin,  $\langle S_1 S_2 \rangle = \langle S_2 \rangle$  and  $\langle S_1 S_3 \rangle = \langle S_3 \rangle$ . In this proposal, the  $\langle S_2 S_3 \rangle$  is measured using a *weak* measurement  $M$  of  $S_2$  at time  $t_2$  and a strong measurement of  $S_3$  at time  $t_3$ .

We consider that between times  $t_1$  and  $t_2$ , and from after the measurement at time  $t_2$  until time  $t_3$ , the system evolves according to the Josephson two-mode Hamiltonian [25,28,30,31]

$$H_I = 2\hbar\kappa\hat{J}_x + \hbar g\hat{J}_z^2. \quad (35)$$

The  $\kappa$  represents the intermode coupling and  $g$  the nonlinear self-interaction due to the medium. Regimes exist where a two-state oscillation (of period  $T_N$ ) takes place (Fig. 3) [28,32]. If the system is prepared in  $|N\rangle_a|0\rangle_b$  at time  $t_1$ , then, in this parameter regime, at a later time  $t_2$  the state vector is to a good approximation given by (apart from an overall phase factor)

$$|\psi(t)\rangle = \cos(t_2 - t_1)|N\rangle_a|0\rangle_b + i\sin(t_2 - t_1)|0\rangle_a|N\rangle_b. \quad (36)$$

Here  $t_i = E_\Delta t'_i/\hbar$  is the time defined in scaled units so that  $t'_i$  is the actual time in seconds and  $E_\Delta$  is the energy splitting of the energy eigenstates  $|N\rangle_a|0\rangle_b \pm |0\rangle_a|N\rangle_b$  under  $H_I$ . In one state,  $|N\rangle_a|0\rangle_b$ , all  $N$  bosons (atoms) are in the mode  $a$  and in the second state,  $|0\rangle_a|N\rangle_b$ , all bosons (atoms) are in the mode  $b$  [28]. As in Fig. 1, we suppose that the system also evolves under this unitary evolution from  $t_2$  (after the measurement  $M$ ) to  $t_3$ . However, between times  $t_1$  and  $t_2$ , we note that the NOON state at time  $t_2$  might be prepared by a different method [21].

The two-time correlation for a measurement of spin  $S_i$  at time  $t_i$  followed by a later measurement of spin  $S_j$  at time  $t_j$  is  $\langle S_i S_j \rangle = \cos[2(t_j - t_i)]$ . This is independent of the outcome at time  $t_i$ , which determines whether the system is projected into  $|N\rangle_a|0\rangle_b$  or  $|0\rangle_a|N\rangle_b$ . Choosing  $t_1 = 0$ ,  $t_2 = \pi/6$ ,  $t_3 = \pi/3$ , it is well known that for this two-time correlation the quantum prediction is  $\text{LG} = 1.5$  which gives a violation of (33) [17]. Alternatively, one can select the values  $t_1 = 0$ ,  $t_2 = \pi/6$  and  $t_3 = 5\pi/12$  in units of  $E_\Delta/\hbar$ , to give a value  $\text{LG} = 1.37$ . Figure 3 shows solutions of the Hamiltonian  $H_I$  for  $N = 5$

and  $g = 2$ , confirming the correlation functions that give violations of the Leggett-Garg inequality in this regime.

In any experimental test of the Leggett-Garg inequalities, the question becomes how to perform the ideal noninvasive measurement at the time  $t_2$ . For any real measurement made at time  $t_2$ , it could be argued that the measurement is not in fact noninvasive, and therefore that the Leggett-Garg inequalities would not apply. The approach taken here, which is well documented in the literature, is to perform a weak measurement at time  $t_2$  [7–9,14]. We will show that the weak measurement in the limit of  $\gamma \rightarrow 0$  can be justified as noninvasive for the input state at time  $t_2$ , and yet yields the required average  $\langle S_2 S_3 \rangle$  for the test of the Leggett-Garg inequality. While this provides a convincing test of the Leggett-Garg macrorealism, we point out that alternative approaches are possible. The ‘‘clumsiness’’ of a measurement can be accounted for, by performing additional measurements and using a modified Leggett-Garg inequality [36,37]. This approach is useful for strong measurements where  $\gamma$  is large, and has been applied to superconducting qubits [36]. The recent papers of Zhou *et al.* [38] and Formaggio *et al.* [39] demonstrate violation of modified Leggett-Garg inequalities based on the assumption of stationarity.

Our proposed experiment is as follows. We assume in this section that we do indeed generate the ideal statistics of the two-state system, so that the evolution is given by Eq. (36). After preparation in the state  $|N\rangle_a|0\rangle_b$  at time  $t_1$ , the system evolves for a time  $t_2 - t_1 = \theta/2$ . The state at time  $t_2$  is therefore

$$|\psi(t_2)\rangle = \cos\frac{\theta}{2}|N\rangle_a|0\rangle_b + i\sin\frac{\theta}{2}|0\rangle_a|N\rangle_b. \quad (37)$$

We then assume the time  $t_3$  is such that  $t_3 - t_2 = \pi/4$ .

In this gedanken experiment, we distinguish between moments that are measured with the weak measurement  $M$  occurring at the time  $t_2$ , or not. The former moments are denoted by the subscript  $M$ . In Fig. 4, the correlation functions  $\langle S_1 S_2 \rangle_M = \langle S_2 \rangle_M$ ,  $\langle S_1 S_3 \rangle_M = \langle S_3 \rangle_M$ , and  $\langle S_2 S_3 \rangle_M$  are plotted versus  $\theta$ . We note that for all  $\gamma$ ,

$$\langle S_2 \rangle_M = \langle S_2 \rangle = -\frac{1}{2\gamma}\langle p \rangle = \cos\theta. \quad (38)$$

This value is independent of  $\gamma$ , i.e., whether the measurement at time  $t_2$  is a weak measurement or a strong measurement. The moment

$$\langle S_2 S_3 \rangle_M = -\frac{1}{2\gamma}\langle p S_3 \rangle = \cos[2(t_3 - t_2)] \quad (39)$$

is also independent of  $\gamma$  and is independent of  $\theta$ . Hence we can write  $\langle S_2 S_3 \rangle = \langle S_2 S_3 \rangle_M$ , although we note that the measurements made with smaller values of  $\gamma$  will have increased statistical error [9]. In this paper, we examine the case where  $t_3 - t_2 = \pi/4$  and hence  $\langle S_2 S_3 \rangle = 0$  for all  $\gamma$ .

A significant difference occurs, however, between  $\langle S_1 S_3 \rangle_M$  and  $\langle S_1 S_3 \rangle$ . We see that without the measurement  $M$  at time  $t_2$ , the moment is

$$\langle S_1 S_3 \rangle = \cos[2(t_3 - t_1)] = -\sin\theta. \quad (40)$$

For a finite  $\gamma$  with the measurement  $M$  occurring at the intermediate time  $t_2$ , we calculate the  $\langle S_1 S_3 \rangle_M$  as follows:

$$\begin{aligned} \langle S_1 S_3 \rangle_M &= P(S_3 \geq 0) - P(S_3 < 0) \\ &= -\sin\theta e^{-2\gamma^2}. \end{aligned} \quad (41)$$

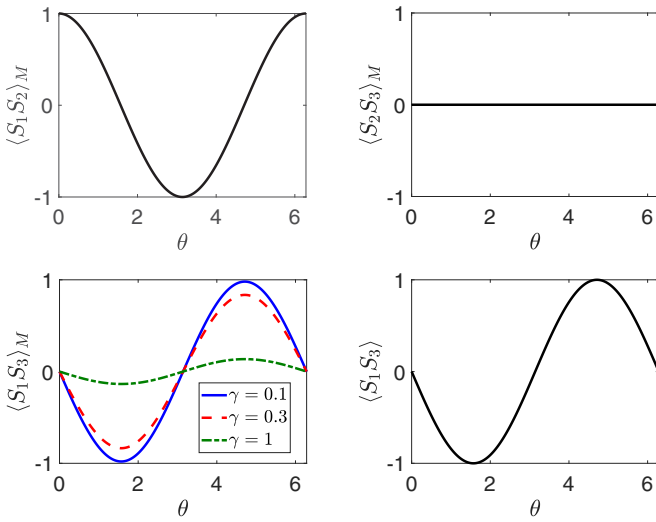


FIG. 4. Correlations associated with the violation of the Leggett-Garg inequality: The graphs show  $\langle S_1 S_2 \rangle_M$ ,  $\langle S_2 S_3 \rangle_M$ ,  $\langle S_1 S_3 \rangle_M$ , and  $\langle S_1 S_3 \rangle$ . The  $\langle S_i S_j \rangle_M$  are evaluated with the measurement at time  $t_2$  as illustrated in Fig. 1. The  $\langle S_1 S_3 \rangle$  is evaluated without a measurement at time  $t_2$ . The averages  $\langle S_1 S_2 \rangle_M$  and  $\langle S_2 S_3 \rangle_M$  are independent of the strength  $\gamma$  of the measurement  $M$ . By contrast,  $\langle S_1 S_3 \rangle_M \rightarrow \langle S_1 S_3 \rangle$  only when  $\gamma \rightarrow 0$ .

The relevant probabilities were defined and calculated in the previous section. In Fig. 4, it is clear that as  $\gamma \rightarrow 0$ ,  $\langle S_1 S_3 \rangle_M \rightarrow \langle S_1 S_3 \rangle$ , indicating a minimal disturbance of the system being measured by the weak measurement. This no-disturbance can be measured in a control experiment, and is used to justify the noninvasive nature of the measurement  $M$  for the purpose of testing the Leggett-Garg inequality, given as

$$\langle S_1 S_2 \rangle_M + \langle S_2 S_3 \rangle_M - \langle S_1 S_3 \rangle_M \leq 1. \quad (42)$$

By contrast, there is a distinct difference between  $\langle S_1 S_3 \rangle_M$  and  $\langle S_1 S_3 \rangle$  for  $\gamma$  large, which corresponds to a strong projective measurement of the spin  $S_2$  at time  $t_2$ . In Fig. 5 we plot the difference  $d_\sigma = \langle S_1 S_3 \rangle_M - \langle S_1 S_3 \rangle$  as the disturbance equality given by Eq. (34) [35,36].

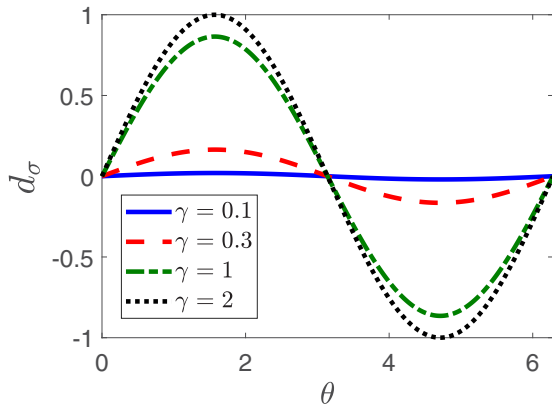


FIG. 5. Measure of disturbance for the weak measurement: We calculate the value of the moments  $\langle S_1 S_3 \rangle_M$  and  $\langle S_1 S_3 \rangle$ . The difference is defined as the disturbance  $d_\sigma$ , plotted here for different values of the measurement strength  $\gamma$ .

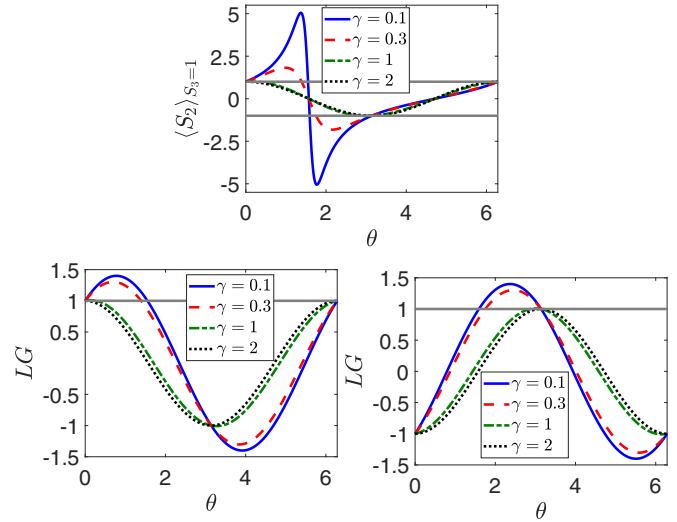


FIG. 6. Correlation between violation of the Leggett-Garg inequality and weak values: The top graph shows  $\langle S_2 \rangle_{S_3=1}$  vs  $\theta$ . In the left lower graph, we plot  $LG = \langle S_1 S_2 \rangle_M + \langle S_2 S_3 \rangle_M - \langle S_1 S_3 \rangle_M$ . In the right lower graph, we plot  $LG = -\langle S_1 S_2 \rangle_M - \langle S_2 S_3 \rangle_M - \langle S_1 S_3 \rangle_M$  defined with the sign of  $S_2$  changed. The Leggett-Garg inequalities are violated when  $LG > 1$ . This corresponds to a weak value regime, observed when  $|\langle S_2 \rangle_{S_3=1}| > 1$ .

In Figs. 6 and 7 we plot the violation of the Leggett-Garg inequality by plotting the Leggett-Garg parameter  $LG = \langle S_1 S_2 \rangle_M + \langle S_2 S_3 \rangle_M - \langle S_1 S_3 \rangle_M$  versus  $\theta$ , for different values of measurement strength  $\gamma$ . At  $\theta/2 = \pi/6$ , the optimal value of  $LG = 1.37$  is possible for small  $\gamma$ . The violation is possible because for small  $\gamma$  the measurement is noninvasive. For sufficiently strong  $\gamma$ , violations are not possible using this particular approach with the inequality (42), because the invasive measurement acts on the system at time  $t_2$  causing a collapse of the wave function into a state of definite spin.

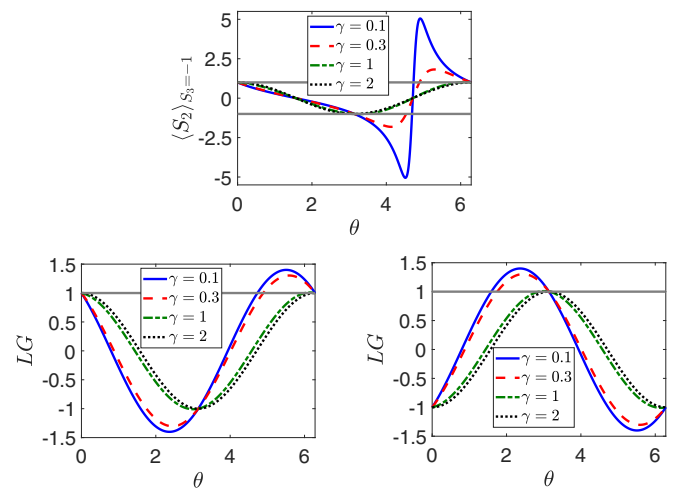


FIG. 7. As for Fig. 6, but here the top graph shows  $\langle S_2 \rangle_{S_3=-1}$ . In the left graph, we plot  $LG = \langle S_1 S_2 \rangle_M - \langle S_2 S_3 \rangle_M + \langle S_1 S_3 \rangle_M$  defined with the sign of  $S_3$  changed. In the right graph, plotted is  $LG = -\langle S_1 S_2 \rangle_M + \langle S_2 S_3 \rangle_M + \langle S_1 S_3 \rangle_M$  defined with the signs of  $S_2$  and  $S_3$  changed.

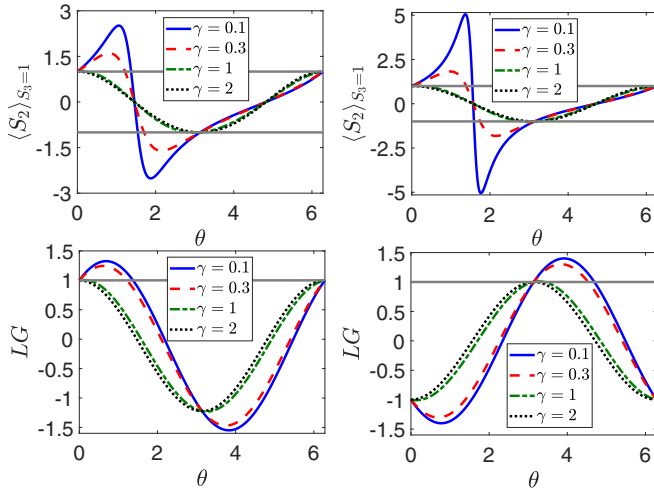


FIG. 8. Violation of the Leggett-Garg inequality and weak values for nonideal evolution after time  $t_2$ : Plots show the weak values and violation of the Leggett-Garg inequality as for Fig. 6, but where the state generated at time  $t_3$  evolves after time  $t_2$  according to the Hamiltonian  $H_I$ . Here  $N = 5$ ,  $g = 2$  (top and lower left), and  $g = 104.43$  (top and lower right). We choose  $t_3 - t_2$  to correspond in real time to one quarter of the two-state oscillation period,  $T_N/4$ .

The violations that occur in the weak measurement regime are directly associated with the presence of weak values [8]. The correlation between the weak values and the violation of the Leggett-Garg inequality is evident in Figs. 6 and 7.

## VI. WEAK VALUES WITH NONIDEAL STATES

### A. Ideal NOON state at time $t_2$

Let us assume an ideal generalized NOON state has been generated at time  $t_2$ . This is not unrealistic for small  $N > 1$ . For example, for  $N = 2$  the Hong-Ou-Mandel effect creates a NOON state [21,22]. Proposals for more macroscopic NOON states use conditioning on measurements of  $\hat{J}_z$  [40]. However, for the generation of the quantum state according to the dynamics of  $H_I$ , the state formed at  $t_3$  is not an ideal NOON state. We examine the effect of this on the weak values and the violation of the Leggett-Garg inequalities.

First, we note that the pure general input state at time  $t_i$  is of the form

$$|\psi\rangle_{\text{in}} = \sum_{m=0}^N d_m |m\rangle_a |N-m\rangle_b \quad (43)$$

given by (4). It is straightforward to show that  $\langle S_i \rangle = -\frac{1}{2\gamma} \langle p \rangle$  for all input states of this type where the total number  $N$  of bosons is fixed. This means that the expression can be used in the more general case for the evaluation of the spin averages. This is also true of the  $\langle S_2 S_3 \rangle$  where the state at time  $t_2$  is the NOON state.

To evaluate the weak values accounting for the general evolution with  $H_I$ , we consider the generalized equations (16)–(19) that allow for a nonideal state at time  $t_3$ . Specifically, the Hamiltonian  $H_I$  is such that the two-mode state  $|0\rangle|N\rangle$  evolves to the state given by  $\sum_n c_n^{(0)} |n\rangle|N-n\rangle$  and two-mode

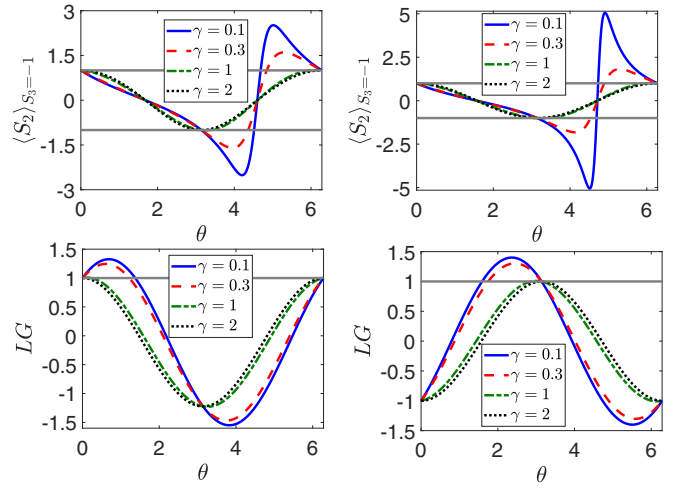


FIG. 9. As for Fig. 8, but with the parameters defined in Fig. 7. Here  $N = 5$ ,  $g = 2$  (top and lower left) and  $g = 104.43$  (top and lower right).

state  $|N\rangle|0\rangle$  evolves to the state given by  $\sum_n c_n^{(N)} |n\rangle|N-n\rangle$  where  $c_n^{(m)}$  are constants. In Figs. 8–10, we plot the predictions for  $\langle \hat{p} \rangle_{S_3=1}$  where we use the values of the precise coefficients  $c_n^{(N)}$  and  $c_n^{(0)}$  generated by the evolution with  $H_I$ , for  $N = 5$  and  $N = 10$ . These have been evaluated by the numerical program that yielded the plots of Fig. 3. The oscillation time is given by  $T_N = \frac{2\pi}{\omega_N}$  where  $\omega_N = 2\hbar g \frac{N}{(N-1)!} (\frac{\kappa}{g})^N$  [28].

The weak values and Leggett-Garg violations are tolerant to the nonideal coefficients, at least for smaller  $N$ . For larger  $N$  corresponding to a BEC, it is known that the parameter regime for oscillation is more difficult to achieve, a phenomenon known as macroscopic quantum self-trapping [26]. This regime may not be impossible however using alternative realizations of the nonlinear Josephson Hamilton [41–43].

### B. Nonideal NOON state at time $t_2$

We conclude by noting that where the state at time  $t_2$  is not an ideal NOON state, evaluating  $\langle S_2 S_3 \rangle$  by way of the measurement given by  $H_M$  is more subtle. To illustrate, let us consider where the two-mode state immediately prior to the measurement at time  $t_2$  is

$$|\psi\rangle = d_{n_a} |n_a\rangle_a |N-n_a\rangle_b + d_{N-n_a} |N-n_a\rangle_a |n_a\rangle_b. \quad (44)$$

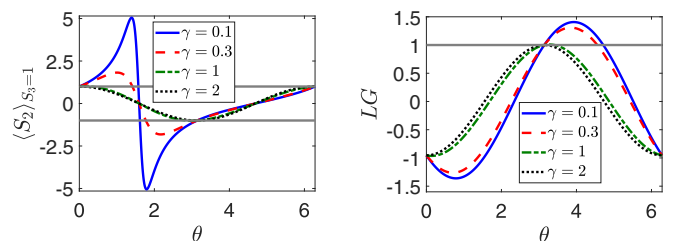


FIG. 10. As for Fig. 8, with parameters defined as for Fig. 6. Here  $N = 10$ ,  $g = 6.6$ .



In this case, the state immediately after the measurement at time  $t_2$  is

$$|\psi\rangle = d_{n_a}|n_a\rangle_a|N - n_a\rangle_b|\gamma e^{i\pi(N-2n_a)/2N}\rangle_c + d_{N-n_a}|N - n_a\rangle_a|n_a\rangle_b|\gamma e^{-i\pi(N-2n_a)/2N}\rangle_c \quad (45)$$

based on Eq. (6). We consider that the state  $|n_a\rangle_a|N - n_a\rangle_b$ , ( $|N - n_a\rangle_a|n_a\rangle_b$ ) evolves as described by a Hamiltonian to the state  $\sum_n c_n^{(n_a)}|n\rangle_a|N - n\rangle_b$  ( $\sum_{n'} c_{n'}^{(N-n_a)}|N - n'\rangle_a|n'\rangle_b$ ) in a time  $t_3 - t_2$ . We then find (see the Appendixes)

$$\langle pS_3 \rangle = -2\gamma \sin\left(\frac{\pi}{2N}(N - 2n_a)\right)\langle S_2S_3 \rangle. \quad (46)$$

This is similar to the earlier result (15) except that the measurement strength is diminished by the sin factor. The calculation indicates that where a general superposition (4) is prepared at time  $t_2$ , the simple weak measurement relation of type (15) does not hold. A more careful analysis is required to place a bound on the value of  $\langle S_2S_3 \rangle$  given the measured  $\langle pS_3 \rangle$ . This is feasible, but will not be addressed in this paper. The result (46) is useful however. This is because in some cases, the mesoscopic superposition state (44) is easier to prepare than the NOON state. It has been shown that the state (44) is generated over shorter time scales than the traditional NOON state, in BEC systems [26,28]. Considerations of time scale are important where decoherence effects are significant.

## VII. CONCLUSION

In summary, we have demonstrated the possibility of detecting quantum weak values using NOON states. We consider a specific nondestructive measurement of the Schwinger spin, defined as the population difference for two levels with a bosonic occupation. This measurement can be realized for atomic systems using an ac Stark shift [24]. The measurement is also applicable to states prepared in polarization modes, as in polarization squeezing experiments, where the observables are defined in terms of Stokes operators [44]. The measurement in the limit of small coupling corresponds to a weak measurement of the Schwinger spin, meaning that it gives the correct average spin for the prepared quantum state, but with a vanishingly small disturbance of the state. By analyzing the case where the measurement is made on a quantum system prepared in a NOON state, we demonstrate how one can detect quantum weak values for the NOON states, for all  $N$ . The detection of the weak values is made possible by a unitary evolution of the quantum system after the measurement, as given by the nonlinear two-mode Josephson Hamiltonian. This gives a way to demonstrate the existence of quantum weak values, for bosonic mesoscopic and macroscopic superposition states.

The work of this paper suggests a Leggett-Garg test of mesorealism or macrorealism using NOON states. In this case, the measurement of a two-time correlation involving the weak measurement is required. We have discussed how to demonstrate the noninvasiveness of the weak measurement for the purpose of a Leggett-Garg test, and have examined the feasibility of the experiment using the Josephson model, with nonideal parameter values.

Finally, we note that regimes associated with more general parameters of the Josephson model do not always lead to a second NOON superposition state being created at the time  $t_3$ . The outcomes for the  $\hat{S}_z$  are not simply  $\pm N$  but can be spread between these values. We comment that tests of quantum weak values and of the Leggett-Garg inequality may still be possible, using the approach of overlapping regions presented in Refs. [33,45].

## ACKNOWLEDGMENTS

We thank L. Drummond for advice on numerical calculations, and P. Drummond and R. Y. Teh for useful suggestions. This research was supported by the Australian Research Council under Grant No. DP140104584. This work was performed in part at Aspen Center for Physics, supported by National Science Foundation Grant No. PHY-1607611.

## APPENDIX A: CALCULATION OF $\langle S_2 \rangle$

We can evaluate  $\langle p \rangle$  from (9), using that  $\hat{p} = \frac{1}{i}(\hat{c} - \hat{c}^\dagger)$ , thus

$$\langle p \rangle = |d_0|^2 \langle \gamma e^{i\pi/2} |p| \gamma e^{i\pi/2} \rangle + |d_N|^2 \langle \gamma e^{-i\pi/2} |p| \gamma e^{-i\pi/2} \rangle. \quad (A1)$$

Next, we use the result for the inner product of coherent states  $\langle \alpha|\beta \rangle = \exp[\alpha^*\beta - |\alpha|^2/2 - |\beta|^2/2]$ , to find

$$\langle \alpha|p|\beta \rangle_a = \frac{1}{i}(\beta - \alpha^*) \exp[\alpha^*\beta - |\alpha|^2/2 - |\beta|^2/2] \quad (A2)$$

and hence

$$\begin{aligned} \langle \gamma e^{-i\pi/2} |p| \gamma e^{-i\pi/2} \rangle &= -2\gamma, \\ \langle \gamma e^{i\pi/2} |p| \gamma e^{i\pi/2} \rangle &= 2\gamma. \end{aligned} \quad (A3)$$

This implies

$$\begin{aligned} \langle p \rangle &= 2\gamma(|d_0|^2 - |d_N|^2) \\ &= -2\gamma \langle S_2 \rangle. \end{aligned} \quad (A4)$$

Here we have used that  $\langle S_2 \rangle = |d_N|^2 - |d_0|^2$ , which is the expectation value of  $S_2$  for the initial two-mode state (4) for the NOON state. We see that

$$\langle S_2 \rangle = -\frac{1}{2\gamma} \langle p \rangle. \quad (A5)$$

The average of  $p$  will give the value for the average of the Schwinger spin of the incident two-mode state.

## APPENDIX B: CALCULATION OF $\langle S_2S_3 \rangle$

We suppose that the Hamiltonian  $H_I$  is such that the two-mode state  $|m\rangle_a|N - m\rangle_b$  evolves to the state  $\sum_n c_n^{(m)}|n\rangle_a|N - n\rangle_b$  where  $c_n^{(m)}$  are constants. The final output state including the meter field is

$$|\psi(t_3)\rangle = \sum_m d_m |\gamma e^{i\pi(N-2m)/2N}\rangle_c \sum_n c_n^{(m)} |n\rangle_a |N - n\rangle_b. \quad (B1)$$

We next evaluate  $\langle pS_3 \rangle$  and compare to  $\langle S_2S_3 \rangle$ . We take the case where prior to the measurement at time  $t_2$  the two-mode

system is in the NOON state:

$$|\psi\rangle = d_0|0\rangle_a|N\rangle_b + d_N|N\rangle_a|0\rangle_b. \quad (\text{B2})$$

At time  $t_3$ , after measurement and after the subsequent evolution, the state is given by Eq. (B1) which we simplify as (13). We evaluate  $\langle pS_3 \rangle = \langle \psi(t_3) | pS_3 | \psi(t_3) \rangle$ , using (A3). Here it is useful to define  $\hat{S}_3|m\rangle_a|N-m\rangle_b = \text{sgn}(2m-N)|m\rangle_a|N-m\rangle_b$  where  $\text{sgn}(S)$  is +1 if  $S \geq 0$ , and -1 otherwise. From (A2) we see that

$$\langle \gamma e^{-i\pi/2} | p | \gamma e^{i\pi/2} \rangle_c = 0 = \langle \gamma e^{i\pi/2} | p | \gamma e^{-i\pi/2} \rangle_c.$$

Hence we obtain

$$\begin{aligned} \langle pS_3 \rangle &= |d_0|^2 2\gamma \left( - \sum_{n < N/2} |c_n^{(0)}|^2 + \sum_{n > N/2} |c_n^{(0)}|^2 \right) \\ &\quad - |d_N|^2 2\gamma \left( - \sum_{n < N/2} |c_n^{(N)}|^2 + \sum_{n > N/2} |c_n^{(N)}|^2 \right). \end{aligned} \quad (\text{B3})$$

Using that  $\langle S_2 S_3 \rangle$  is given by Eq. (14), we find

$$\langle S_2 S_3 \rangle = -\frac{1}{2\gamma} \langle pS_3 \rangle. \quad (\text{B4})$$

### APPENDIX C: CALCULATION FOR THE NONIDEAL CASE

We consider that the state  $|n_a\rangle_a|N-n_a\rangle_b$  evolves as described above by a Hamiltonian  $H_I$  to the state  $\sum_n c_n^{(n_a)}|n\rangle_a|N-n\rangle_b$  in a time  $t_3 - t_2$ . Similarly, the state  $|N-n_a\rangle_a|n_a\rangle_b$  evolves to  $\sum_{n'} c_{n'}^{(N-n_a)}|N-n'\rangle_a|n'\rangle_b$ . Hence

$$\begin{aligned} S_3 |\psi(t_3)\rangle &= d_{n_a} |\gamma e^{+i\pi(N-2n_a)/2N}\rangle_c \\ &\quad \times \sum_n c_n^{(n_a)} \text{sgn}(2n-N) |n\rangle_a |N-n\rangle_b \\ &\quad + d_{N-n_a} |\gamma e^{-i\pi(N-2n_a)/2N}\rangle_c \\ &\quad \times \sum_{n'} c_{n'}^{(N-n_a)} \text{sgn}(N-2n') |N-n'\rangle_a |n'\rangle_b. \end{aligned} \quad (\text{C1})$$

Therefore

$$\begin{aligned} \langle pS_3 \rangle &= 2\gamma \sin\left(\frac{\pi}{2N}(N-2n_a)\right) \\ &\quad \times \left( |d_{n_a}|^2 \sum_n |c_n^{(n_a)}|^2 \text{sgn}(2n-N) \right. \\ &\quad \left. - |d_{N-n_a}|^2 \sum_{n'} |c_{n'}^{(N-n_a)}|^2 \text{sgn}(N-2n') \right) \\ &= -2\gamma \sin\left(\frac{\pi}{2N}(N-2n_a)\right) \langle S_2 S_3 \rangle. \end{aligned} \quad (\text{C2})$$

- 
- [1] Y. Aharonov, D. Z. Albert, and L. Vaidman, *Phys. Rev. Lett.* **60**, 1351 (1988).
- [2] Y. Aharonov and L. Vaidman, *Phys. Rev. A* **41**, 11 (1990).
- [3] J. Dressel, M. Malik, F. M. Miatto, A. N. Jordan, and R. W. Boyd, *Rev. Mod. Phys.* **86**, 307 (2014); O. Hosten and P. Kwiat, *Science* **319**, 787 (2008); P. Dixon, D. Starling, A. Jordan, and J. Howell, *Phys. Rev. Lett.* **102**, 173601 (2009).
- [4] G. J. Pryde, J. L. O'Brien, A. G. White, T. C. Ralph, and H. M. Wiseman, *Phys. Rev. Lett.* **94**, 220405 (2005); G. J. Pryde, J. L. O'Brien, A. G. White, S. D. Bartlett, and T. C. Ralph, *ibid.* **92**, 190402 (2004).
- [5] N. W. M. Ritchie, J. G. Story, and R. G. Hulet, *Phys. Rev. Lett.* **66**, 1107 (1991).
- [6] J. P. Groen, D. Ristè, L. Tornberg, J. Cramer, P. C. de Groot, T. Picot, G. Johansson, and L. DiCarlo, *Phys. Rev. Lett.* **111**, 090506 (2013).
- [7] R. Ruskov, A. N. Korotkov, and A. Mizel, *Phys. Rev. Lett.* **96**, 200404 (2006).
- [8] A. N. Jordan, A. N. Korotkov, and M. Buttiker, *Phys. Rev. Lett.* **97**, 026805 (2006). N. S. Williams and A. N. Jordan, *ibid.* **100**, 026804 (2008).
- [9] M. E. Goggin, M. P. Almeida, M. Barbieri, B. P. Lanyon, J. L. O'Brien, A. G. White, and G. J. Pryde, *Proc. Natl. Acad. Sci. USA* **108**, 1256 (2011).
- [10] C. Emary, N. Lambert, and F. Nori, *Rep. Prog. Phys.* **77**, 016001 (2014).
- [11] T. C. White *et al.*, *NPJ Quantum Inf.* **2**, 15022 (2016).
- [12] B. L. Higgins, M. S. Palsson, G. Y. Xiang, H. M. Wiseman, and G. J. Pryde, *Phys. Rev. A* **91**, 012113 (2015).
- [13] Y. Suzuki, M. Iinuma, and H. F. Hofmann, *New J. Phys.* **14**, 103022 (2012).
- [14] A. Palacios-Laloy, F. Mallet, F. Nguyen, P. Bertet, D. Vion, D. Esteve, and A. N. Korotkov, *Nat. Phys.* **6**, 442 (2010).
- [15] J. Dressel, C. J. Broadbent, J. C. Howell, and A. N. Jordan, *Phys. Rev. Lett.* **106**, 040402 (2011); J.-S. Xu, C.-F. Li, X.-B. Zou, and G.-C. Guo, *Sci. Rep.* **1**, 101 (2011); V. Athalye, S. S. Roy, and T. S. Mahesh, *Phys. Rev. Lett.* **107**, 130402 (2011); A. M. Souza, I. S. Oliveira, and R. S. Sarthour, *New J. Phys.* **13**, 053023 (2011); H. Katiyar, A. Shukla, K. R. Rao, and T. S. Mahesh, *Phys. Rev. A* **87**, 052102 (2013); R. E. George, L. M. Robledo, O. J. E. Maroney, M. S. Blok, H. Bernien, M. L. Markham, D. J. Twitchen, J. J. L. Morton, G. A. D. Briggs, and R. Hanson, *Proc. Natl. Acad. Sci. USA* **110**, 3777 (2013).
- [16] H. M. Wiseman, *Phys. Lett. A* **311**, 285 (2003); J. L. Garretson, H. M. Wiseman, D. T. Pope, and D. T. Pegg, *J. Opt. B* **6**, S506 (2004); Y. Aharonov, A. Botero, S. Popescu, B. Reznik, and J. Tollaksen, *Phys. Lett. A* **301**, 130 (2002); S. E. Ahnert and M. C. Payne, *Phys. Rev. A* **70**, 042102 (2004).
- [17] A. J. Leggett and A. Garg, *Phys. Rev. Lett.* **54**, 857 (1985).
- [18] A. Asadian, C. Brukner, and P. Rabl, *Phys. Rev. Lett.* **112**, 190402 (2014).
- [19] C. Budroni, G. Vitagliano, G. Colangelo, R. J. Sewell, O. Gühne, G. Tóth, and M. W. Mitchell, *Phys. Rev. Lett.* **115**, 200403 (2015).
- [20] S. Huang and G. S. Agarwal, *New J. Phys.* **17**, 093032 (2015).

- [21] J. P. Dowling, *Contemp. Phys.* **49**, 125 (2008); I. Afek, O. Ambar, and Y. Silberberg, *Science* **328**, 879 (2010); M. W. Mitchell, J. S. Lundeen, and A. M. Steinberg, *Nature (London)* **429**, 161 (2004); P. Walther, J.-W. Pan, M. Aspelmeyer, R. Ursin, S. Gasparoni, and A. Zeilinger, *ibid.* **429**, 158 (2004); S. Slussarenko, M. M. Weston, H. M. Chrzanowski, L. K. Shalm, V. B. Verma, S. W. Nam, and G. J. Pryde, *Nat. Photon.* **11**, 700 (2017).
- [22] R. Lopes, A. Imanaliev, A. Aspect, M. Cheneau, D. Boiron, and C. I. Westbrook, *Nature (London)* **520**, 66 (2015); R. J. Lewis-Swan and K. V. Kheruntsyan, *Nat. Commun.* **5**, 3752 (2014).
- [23] A. Blais, R. S. Huang, A. Wallraff, S. M. Girvin, and R. J. Schoelkopf, *Phys. Rev. A* **69**, 062320 (2004); A. Wallraff, D. I. Schuster, A. Blais, L. Frunzio, R.-S. Huang, J. Majer, S. Kumar, S. M. Girvin, and R. J. Schoelkopf, *Nature (London)* **431**, 162 (2004).
- [24] E. O. Ilo-Okeke and T. Byrnes, *Phys. Rev. Lett.* **112**, 233602 (2014).
- [25] J. Estève, C. Gross, A. Weller, S. Giovanazzi, and M. K. Oberthaler, *Nature (London)* **455**, 1216 (2008).
- [26] M. Albiez, R. Gati, J. Fölling, S. Hunsmann, M. Cristiani, and M. K. Oberthaler, *Phys. Rev. Lett.* **95**, 010402 (2005).
- [27] B. Opanchuk, L. Rosales-Zárate, R. Y. Teh, and M. D. Reid, *Phys. Rev. A* **94**, 062125 (2016).
- [28] L. D. Carr, D. R. Dounas-Frazer, and M. A. Garcia-March, *Europhys. Lett.* **90**, 10005 (2010); D. R. Dounas-Frazer, A. M. Hermundstad, and L. D. Carr, *Phys. Rev. Lett.* **99**, 200402 (2007).
- [29] Q. Y. He, P. D. Drummond, M. K. Olsen, and M. D. Reid, *Phys. Rev. A* **86**, 023626 (2012); B. Opanchuk, Q. Y. He, M. D. Reid, and P. D. Drummond, *ibid.* **86**, 023625 (2012).
- [30] M. J. Steel and M. J. Collett, *Phys. Rev. A* **57**, 2920 (1998); H. J. Lipkin, N. Meshkov, and A. J. Glick, *Nucl. Phys.* **62**, 188 (1965).
- [31] C. Gross, T. Zibold, E. Nicklas, J. Estève, and M. K. Oberthaler, *Nature (London)* **464**, 1165 (2010); M. F. Riedel, P. Böhi, Y. Li, T. W. Hänsch, A. Sinatra, and P. Treutlein, *ibid.* **464**, 1170 (2010); M. Egorov, R. P. Anderson, V. Ivannikov, B. Opanchuk, P. Drummond, B. V. Hall, and A. I. Sidorov, *Phys. Rev. A* **84**, 021605 (2011).
- [32] G. J. Milburn, J. Corney, E. M. Wright, and D. F. Walls, *Phys. Rev. A* **55**, 4318 (1997); J. I. Cirac, M. Lewenstein, K. Mølmer, and P. Zoller, *ibid.* **57**, 1208 (1998); J. A. Dunningham and K. Burnett, *J. Mod. Opt.* **48**, 1837 (2001); D. Gordon and C. M. Savage, *Phys. Rev. A* **59**, 4623 (1999); Y. Zhou, H. Zhai, R. Lü, Z. Xu, and L. Chang, *ibid.* **67**, 043606 (2003); T. J. Haigh, A. J. Ferris, and M. K. Olsen, *Opt. Commun.* **283**, 3540 (2010); K. Pawłowski, M. Fadel, P. Treutlein, Y. Castin, and A. Sinatra, *Phys. Rev. A* **95**, 063609 (2017).
- [33] L. Rosales-Zárate, B. Opanchuk, Q. Y. He, and M. D. Reid, [arXiv:1612.05726](https://arxiv.org/abs/1612.05726) [Phys. Rev. A (to be published)].
- [34] A. N. Jordan and M. Büttiker, *Phys. Rev. B* **71**, 125333 (2005); A. N. Jordan and A. N. Korotkov, *ibid.* **74**, 085307 (2006).
- [35] C.-M. Li, N. Lambert, Y.-N. Chen, G.-Y. Chen, and F. Nori, *Sci. Rep.* **2**, 885 (2012); J. Kofler and C. Brukner, *Phys. Rev. A* **87**, 052115 (2013); L. Clemente and J. Kofler, *ibid.* **91**, 062103 (2015); *Phys. Rev. Lett.* **116**, 150401 (2016); K. Wang, G. C. Knee, X. Zhan, Z. Bian, J. Li, and P. Xue, *Phys. Rev. A* **95**, 032122 (2017).
- [36] G. C. Knee, K. Kakuyanagi, M.-C. Yeh, Y. Matsuzaki, H. Toida, H. Yamaguchi, S. Saito, A. J. Leggett, and W. J. Munro, *Nat. Commun.* **7**, 13253 (2016).
- [37] G. Vitagliano, Quantifying the clumsiness of QND measurements in Leggett-Garg tests, presented at Workshop in Temporal Quantum Correlations and Steering, Siegen (2016).
- [38] Z.-Q. Zhou, S. F. Huelga, C.-F. Li, and G.-C. Guo, *Phys. Rev. Lett.* **115**, 113002 (2015).
- [39] J. A. Formaggio, D. I. Kaiser, M. M. Murskyj, and T. E. Weiss, *Phys. Rev. Lett.* **117**, 050402 (2016).
- [40] M. Stobinska, F. Töppel, P. Sekatski, A. Buraczewski, M. Żukowski, M. V. Chekhova, G. Leuchs, and N. Gisin, *Phys. Rev. A* **86**, 063823 (2012); T. Sh. Iskhakov, K. Yu Spasibko, M. V. Chekhova, and G. Leuchs, *New J. Phys.* **15**, 093036 (2013); K. Yu Spasibko, F. Töppel, T. Sh. Iskhakov, M. Stobińska, M. V. Chekhova, and G. Leuchs, *ibid.* **16**, 013025 (2014); G. J. Pryde and A. G. White, *Phys. Rev. A* **68**, 052315 (2003); A. E. B. Nielsen and K. Mølmer, *ibid.* **75**, 063803 (2007).
- [41] K. K. Likharev, *Rev. Mod. Phys.* **51**, 101 (1979); C. Wang *et al.*, *Science* **352**, 1087 (2016); S. Zeytinoglu, M. Pechal, S. Berger, A. A. Abdumalikov, A. Wallraff, and S. Filipp, *Phys. Rev. A* **91**, 043846 (2015); C. Eichler, Y. Salathe, J. Mlynek, S. Schmidt, and A. Wallraff, *Phys. Rev. Lett.* **113**, 110502 (2014).
- [42] S. Backhaus, S. Pereverzev, R. W. Simmonds, A. Loshak, J. C. Davis, and R. E. Packard, *Nature (London)* **392**, 687 (1998).
- [43] M. Abbarchi *et al.*, *Nat. Phys.* **9**, 275 (2013).
- [44] N. Korolkova, G. Leuchs, R. Loudon, T. C. Ralph, and C. Silberhorn, *Phys. Rev. A* **65**, 052306 (2002).
- [45] E. G. Cavalcanti and M. D. Reid, *Phys. Rev. Lett.* **97**, 170405 (2006); *Phys. Rev. A* **77**, 062108 (2008); C. Marquardt, U. L. Andersen, G. Leuchs, Y. Takeno, M. Yukawa, H. Yonezawa, and A. Furusawa, *ibid.* **76**, 030101(R) (2007).